01.5;06.3

Light-induced generation of dark dissipative envelope solitons in an active ring resonator based on a bicomponent magnonic crystal „ferromagnetic–semiconductor“

© A.S. Bir[1], M.A. Morozova[1], D.V. Romanenko[1], S.A. Nikitov[1,2], S.V. Grishin[1]

[1] Saratov National Research State University, Saratov, Russia
[2] Kotelnikov Institute of Radio Engineering and Electronics, Russian Academy of Sciences, Moscow, Russia
E-mail: sergrsh@yandex.ru

Received August 3, 2023
Revised September 8, 2023
Accepted September 29, 2023

Light-induced generation of the dark dissipative envelope solitons has been carried out in a microwave active ring resonator containing a nonlinear bicomponent magnonic crystal (BMC). The BMC is an yttrium iron garnet film, on the surface of which there is a one-dimensional periodic structure of thin semiconductor strips of silicon (Si). Illumination of the BMC with a laser beam leads to a shift in the band gap frequency of the BMC due to the change in the Si conductivity. It is a cause the generation of dark (gray) dissipative envelope solitons through the four-wave nonlinear spin-wave interactions.

Keywords: magnonic crystals, semiconductors, dissipative solitons, spin waves.

DOI: 10.61011/TPL.2023.11.57203.19701

Magnon spintronics, which studies the interaction between magnons (quanta of spin waves, SWs) and free carriers of spin-polarized or electric currents, is one of the currently relevant research trends in magnonics [1]. Ferrite-semiconductor structures [2–11] and ferro- or antiferromagnetic semiconductors [12] supporting the interaction of traveling SWs with free carriers are of interest in the context of design of spintronic devices operating in both microwave and terahertz ranges. The amplification of traveling magnetostatic surface SWs (MSSWs) in a ferrite-semiconductor structure in a constant electric field was examined in [2,3]. In addition, the Bragg resonance in the spectrum of traveling SWs was controlled efficiently in [4] by applying a constant electric field to a periodic (Bragg) grating formed on the surface of a ferrite film (bicomponent magnonic crystal, BMC). It was demonstrated in [5] that Bragg resonances in the spectrum of traveling SWs may also be controlled by an electric field in a single-component magnonic crystal. In this study, a periodic structure in the form of columns and grooves on the surface of a ferrite film was adjacent to a semiconductor film to which the electric field was applied.

Nonlinear effects in the form of bright envelope solitons in ferrite-semiconductor structures were examined [6–9] alongside with linear ones. Electrical control over bright envelope solitons traveling in a ferrite film with a semiconductor film on its surface [6–8] and over Bragg envelope solitons in a single-component magnonic crystal adjacent to a semiconductor film [9] was demonstrated.

The density of carriers in a semiconductor may be controlled both by an applied constant electric field and by optical (laser) radiation that induces a constant electric field in a photosensitive semiconductor [10]. It was demonstrated in [11] that laser radiation incident onto a ferrite-semiconductor structure allows one to control the nonreciprocity of propagating MSSWs. However, the potential for control over envelope solitons and their photoexcitation has not been examined. In the present study, experimental data on photoexcitation of dark envelope solitons in a BMC in the feedback circuit of an active ring resonator are reported.

Figure 1 presents the diagram of an active ring resonator that features a one-dimensional (1D) BMC, a TWT (traveling-wave tube) amplifier, and an adjustable attenuator. The 1D BMC was constructed based on an yttrium iron garnet (YIG) film $d = 10\,\mu$m in thickness and 4 mm in width with a saturation magnetization of $4\pi M_0 = 1750$ G and a ferromagnetic resonance linewidth of 0.5 Oe measured at a frequency of 9.2 GHz. A periodic structure of silicon strips with a period of $200\,\mu$m was formed lithographically on the YIG film surface. Semiconductor strips had a width of $100\,\mu$m, a thickness of 200 nm, and a conductivity of $5 \cdot 10^{-7}\,\Omega^{-1} \cdot \mathrm{cm}^{-1}$. The 1D periodic structure was 5 mm in length. A red laser operating at 830 nm with an intensity varying within the 0–400 mW range was used in the experiment. It was focused into a spot 4 mm in diameter. Since the indicated wavelength exceeds the band gap width of silicon, a photoresistive effect was induced under irradiation of silicon by this red laser. Therefore, the conductivity of silicon depended on the laser radiation intensity. Input and output microstrip transducers were used to excite and receive an MSSW propagating in the 1D BMC. Each of them had a width of $30\,\mu$m and a length of 6 mm. The distance between them was 6 mm. External constant magnetic field H_0 was applied tangentially to the 1D BMC surface and parallel to microstrip transducers. The field strength was set to $H_0 = 1520$ Oe, since the BMC was to

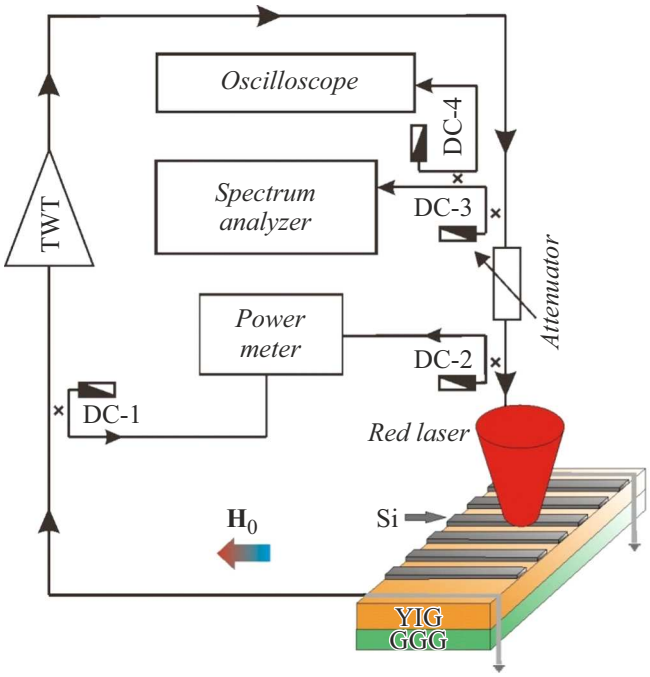

Figure 1. Block diagram of the microwave ring generator of dark dissipative envelope solitons.

be operated at frequencies above 5 GHz where the influence of irradiated Si strips on a traveling MSSW in the YIG film was the most pronounced. In addition, only four-wave nonlinear spin-wave interactions may progress in the YIG film at this strength of an external constant magnetic field [13]. The TWT amplifier was operated in the linear signal amplification mode and served to compensate losses in the ring. The signal power level at the 1D BMC input was controlled by the adjustable attenuator and monitored with a power meter. A microwave signal generated in the ring was fed to the inputs of a spectrum analyzer and a real-time oscilloscope for analysis and subsequent processing.

Figure 2 shows the amplitude-frequency response characteristics of the 1D BMC measured outside of the ring in the linear mode both without laser irradiation and under irradiation. It follows from the data in Fig. 2 that the MSSW spectrum measured without laser irradiation has a stopband (cyan-colored; a color version of the figure is provided in the online version of the paper) in the low-frequency region. The center frequency of this stopband ($f_c = 6.3645$ GHz) corresponds to MSSW wavenumber $k_c = 148\,\text{cm}^{-1}$, which is close to wavenumber $k_{br1} = 157\,\text{cm}^{-1}$ of the first Bragg resonance (see the inset in Fig. 2). A slight discrepancy between wavenumbers k_c and k_{br1} and the corresponding frequencies f_c and $f_{br1} = 6.3707$ GHz may be attributed to a reduction in strength of the internal magnetic field of the YIG film due to the emergence of a demagnetization field in a film constrained in width [14]. Under laser irradiation at an intensity of 136 mW, the mentioned stopband (the first band gap of the 1D BMC) shifts upward in frequency; at the same time, a second stopband (green-colored), which apparently corresponds to the second Bragg resonance with $k_{br2} = 314\,\text{cm}^{-1}$, emerges in the higher-frequency region of the MSSW spectrum. The upward frequency shift of the first Bragg resonance is attributable to the fact that both the electric field in Si strips and the density of photoexcited carriers (electrons) grow with increasing intensity of laser radiation [10]. Owing to this enhancement of carrier density, Si strips become more conductive and acquire near-metallic properties. The dispersion characteristic of an MSSW traveling in a free YIG film then becomes similar to the dispersion characteristic of an MSSW traveling in a YIG film with a metallic screen positioned near its surface [15]. If $k_{br1} = \text{const}$, the enhancement of conductivity of Si strips results in an upward shift of the frequency corresponding to the first Bragg wavenumber. It should be noted that thermal heating accompanying the process of laser irradiation of the YIG film does not dominate over the conductivity dependence of the frequency of the first Bragg resonance: if this was not so, a downward shift of this frequency would be observed instead of an upward one.

Figure 3 presents the experimental data on generation of periodic sequences of dark dissipative envelope solitons with the 1D BMC introduced into the feedback circuit of the active ring resonator. It follows from Figs. 3, *a*, *c* that a multi-frequency microwave signal with carrier frequency $f_{osc1} = 6.3985$ GHz, which is close to one of the primary peaks of the amplitude-frequency response characteristic of the 1D BMC (Fig. 2), is generated in the self-oscillating system without laser irradiation. Satellites characterized by automodulation frequency $f_{am} = 3.75$ MHz are located on both sides of the carrier frequency. Automodulation is

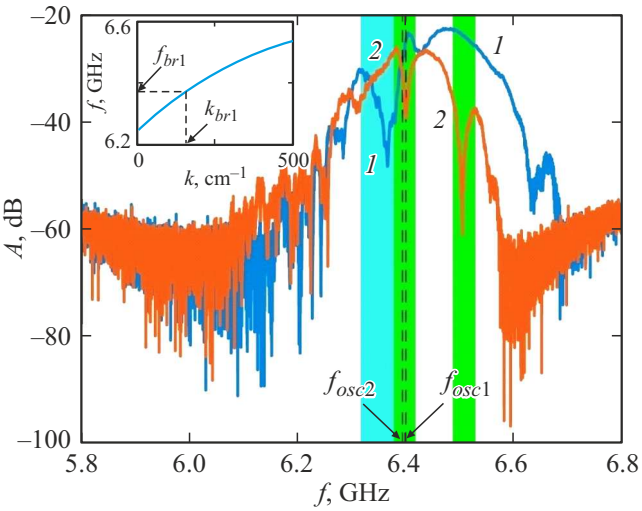

Figure 2. Amplitude-frequency response characteristics of the 1D BMC based on the YIG film with a periodic structure of semiconductor strips measured without laser irradiation (*1*) and under irradiation at an intensity of 136 mW (*2*). The calculated dispersion characteristic of an MSSW for a free YIG film with $d = 10\,\mu$m, $4\pi M_0 = 1750$ G, and $H_0 = 1520$ Oe is shown in the inset.

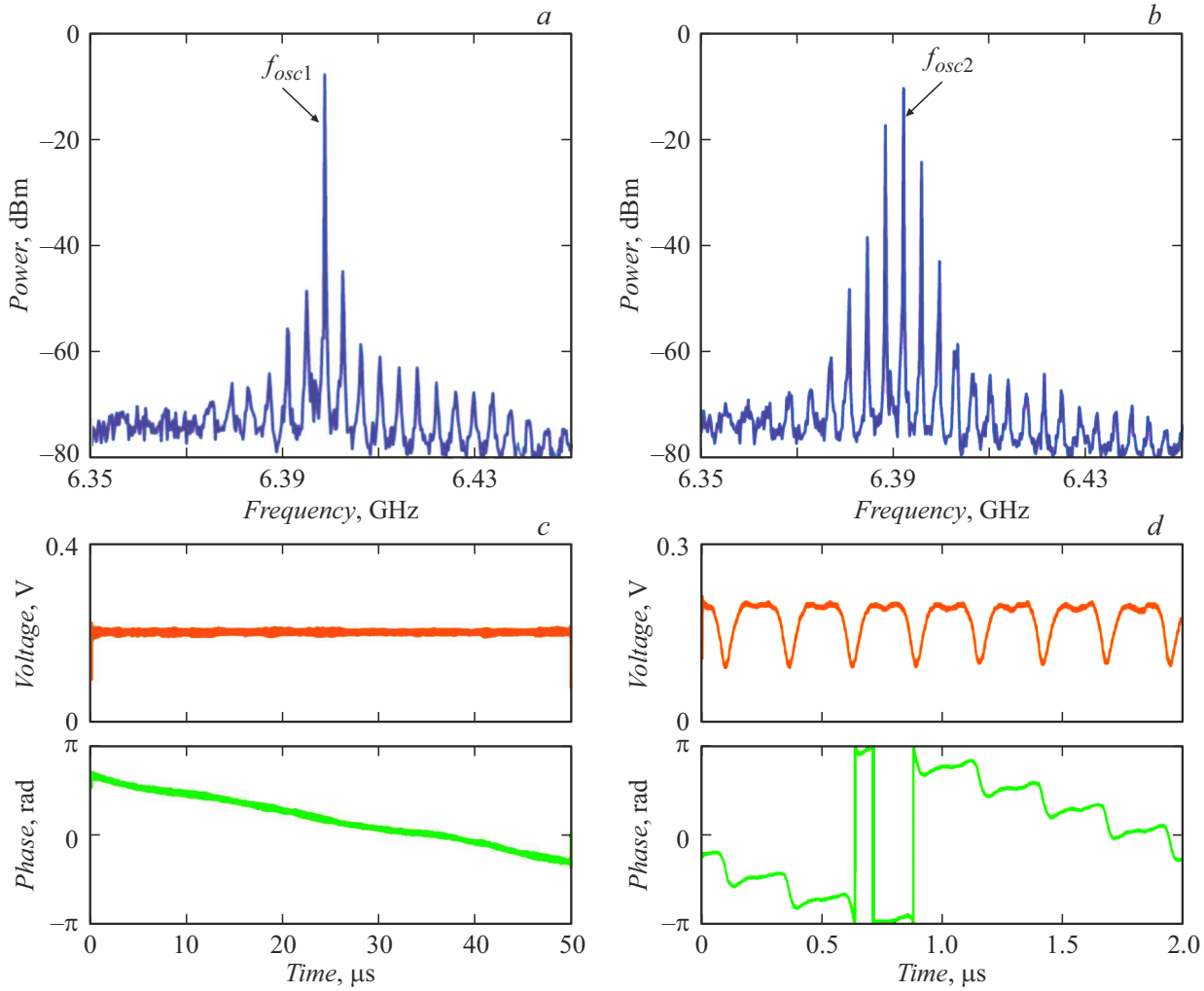

Figure 3. Power spectra (a, b) and amplitude (upper panels) and phase (lower panels) envelope profiles (c, d) of a microwave signal generated in the active ring resonator with the 1D BMC without laser irradiation (a, c) and under irradiation (b, d) at an intensity of 136 mW.

the result of four-wave nonlinear spin-wave interactions in the 1D BMC, since parametric three-wave MSSW decay processes are forbidden at these frequencies. However, the power of satellites with the highest amplitude is 40 dB lower than the carrier power level; therefore, the envelope of this multi-frequency microwave signal has an almost constant amplitude.

The pattern changes when continuous-wave laser radiation with a power of 136 mW is incident on Si strips (Figs. $3, b, d$). The carrier frequency then shifts slightly downward to $f_{osc2} = 6.392$ GHz, residing at the low-frequency edge of the first band gap of the 1D BMC. The amplitudes of satellites in the signal power spectrum increase significantly as a result, and a periodic sequence of dark envelope solitons forms in the time domain. Their amplitude does not decrease strictly to zero, and the phase does not undergo a shift by π at the soliton center; therefore, these dark solitons are gray envelope solitons [13]. The repetition rate in the pulse sequence corresponds to frequency f_{am}, and their duration is 49 ns. This duration was determined at the 1.4-fold amplitude enhancement (relative to the minimum value) level and does not exceed the time of pulse transit through the BMC. It should be noted that both bright and dark envelope solitons were obtained in earlier experiments with a single-component magnonic crystal located outside of the ring when either short microwave pulses [16] or a monochromatic microwave signal of a varying power level [17] were fed to the magnonic crystal input. It was found that bright envelope solitons formed either from short MSSW pulses [16] or due to the development of modulation instability at backward bulk magnetostatic spin waves [17] when the carrier frequency of microwave pulses or the frequency of a monochromatic microwave signal fell on the high-frequency slope of the Bragg resonance. At the same time, dark envelope solitons formed when the frequency of a monochromatic microwave signal fell on the low-frequency slope of the Bragg resonance [17]. Thus, the observed

photoexcitation of dark envelope solitons in a self-oscillator on the low-frequency slope of the Bragg resonance does not contradict literature data.

The obtained results may find application in the development of controllable pulse signal sources for magnon logic and spintronic systems.

Funding

This study was supported by a grant from the Russian Science Foundation, project № 23-79-30027 (https://rscf.ru/project/23-79-30027/).

Conflict of interest

The authors declare that they have no conflict of interest.

References

[1] A.V. Chumak, V.I. Vasyuchka, A.A. Serga, B. Hillebrands, Nat. Phys., **11** (6), 453 (2015). DOI: 10.1038/nphys3347
[2] V.P. Lukomskii, Yu.A. Tsvirko, Fiz. Tverd. Tela, **15** (3), 700 (1973) (in Russian).
[3] Yu.V. Gulyaev, P.E. Zil'berman, Radiotekh. Elektron., **23** (5), 897 (1978) (in Russian).
[4] Yu.V. Gulyaev, S.A. Nikitov, Fiz. Tverd. Tela, **25** (8), 2515 (1983) (in Russian).
[5] M.A. Morozova, D.V. Romanenko, A.A. Serdobintsev, O.V. Matveev, Yu.P. Sharaevskii, S.A. Nikitov, J. Magn. Magn. Mater., **514** (15), 167202 (2020). DOI: 10.1016/j.jmmm.2020.167202
[6] A.S. Kindyak, Tech. Phys., **44** (6), 715 (1999). DOI: 10.1134/1.1259449.
[7] A.S. Kindyak, V.V. Kindyak, Phys. Solid State, **41** (7), 1162 (1999). DOI: 10.1134/1.1130972.
[8] A.S. Kindyak, A.D. Boardman, V.V. Kindyak, J. Magn. Magn. Mater., **253** (1-2), 8 (2002). DOI: 10.1016/S0304-8853(01)00195-0
[9] O.V. Matveev, D.V. Romanenko, M.A. Morozova, JETP Lett., **115** (6), 343 (2022). DOI: 10.1134/S0021364022100228.
[10] A.S. Kindyak, Pis'ma Zh. Tekh. Fiz., **21** (19), 68 (1995) (in Russian).
[11] A.V. Sadovnikov, E.N. Beginin, S.E. Sheshukova, Yu.P. Sharaevskii, A.I. Stognij, N.N. Novitski, V.K. Sakharov, Yu.V. Khivintsev, S.A. Nikitov, Phys. Rev. B, **99** (5), 054424 (2019). DOI: 10.1103/PhysRevB.99. 054424
[12] S.V. Grishin, A.V. Bogomolova, S.A. Nikitov, Tech. Phys. Lett., **48** (3), 37 (2022). DOI: 10.21883/TPL.2022.03.52881.18955.
[13] M. Wu, Solid State Phys., **62**, 163 (2010). DOI: 10.1016/B978-0-12-374293-3.00003-1
[14] A.V. Sadovnikov, C.S. Davies, S.V. Grishin, V.V. Kruglyak, D.V. Romanenko, Yu.P. Sharaevskii, S.A. Nikitov, Appl. Phys. Lett., **106** (19), 192406 (2015). DOI: 10.1063/1.4921206
[15] A.S. Kindyak, Zh. Tekh. Fiz., **64** (11), 99 (1994) (in Russian).
[16] A.V. Drozdovskii, M.A. Cherkasskii, A.B. Ustinov, N.G. Kovshikov, B.A. Kalinikos, JETP Lett., **91** (1), 16 (2010). DOI: 10.1134/S0021364010010042.
[17] A.V. Drozdovskii, B.A. Kalinikos, JETP Lett., **95** (7), 357 (2012). DOI: 10.1134/S0021364012070041.

Translated by D.Safin